FULL PAPER

Dipyrromethane-Based PGeP Pincer Methylgermyl and Methoxidogermyl Nickel and Palladium Complexes

Javier A. Cabeza, *[a] Pablo García-Álvarez,[a] Carlos J. Laglera-Gándara[a] and Enrique Pérez-Carreño[b]

Dedicated to the memory of Prof. Víctor Riera, a pioneer of the Spanish Organometallic Chemistry, a great teacher and a great mentor

[a] Prof. J. A. Cabeza, Prof. P. García-Ávarez, Dr. C. J. Laglera-Gándara
Centro de Innovación en Química Avanzada (ORFEO-CINQA)
Departamento de Química Orgánica e Inorgánica and
Universidad de Oviedo
33071 Oviedo, Spain
E-mail: jac@uniovi.es
https://www.unioviedo.es/jaclab/jacweb/jac
[b] Prof. E. Pérez-Carreño
Departamento de Química Física y Analítica
Universidad de Oviedo
33071 Oviedo, Spain

Supporting information for this article is given via a link at the end of the document.

Abstract: The dipyrromethane-based chloridogermyl complexes [MCl{κ^3*P*,Ge,*P*-GeCl(pyrmP^{i}Pr$_2$)$_2$CMe$_2$}] (**1$_M$**; M = Ni, Pd; (pyrmP^{i}Pr$_2$)$_2$CMe$_2$ = 5,5'-dimethyl-2,2'-bis(di-isopropylphosphanylmethyl)dipyrromethane-1,1'-diyl) reacted with one or more equivalents of LiOMe to give the monosubstituted complexes [MCl{κ^3*P*,Ge,*P*-Ge(OMe)(pyrmP^{i}Pr$_2$)$_2$CMe$_2$}] (**2$_{M\text{-}OMe}$**; M = Ni, Pd). However, analogous treatments of complexes **1$_M$** with LiMe afforded the dimethyl complexes [MMe{κ^3*P*,Ge,*P*-GeMe(pyrmP^{i}Pr$_2$)$_2$CMe$_2$}] (**3$_{M\text{-}Me}$**; M = Ni, Pd). The monomethyl complexes [MCl{κ^3*P*,Ge,*P*-GeMe(pyrmP^{i}Pr$_2$)$_2$CMe$_2$}] (**2$_{M\text{-}Me}$**; M = Ni, Pd), which were identified as intermediates in the syntheses of **3$_{M\text{-}Me}$**, were satisfactorily prepared by treating **3$_{M\text{-}Me}$** with HCl. The regioselectivities of these reactions have been rationalized with DFT calculations.

Introduction

The recent availability of metal-free PGeP germylenes (Figure 1)[1-8] has allowed an advance of the coordination chemistry of PGeP pincer complexes.[1] In fact, some of these germylenes have already led to transition metal (TM) complexes containing either PGeP pincer germylene ligands (just by simple coordination)[7,8] or PGeP pincer germyl ligands (by insertion of the Ge atom into an M–Cl bond of the metal precursor).[2-4,8-11] A few PGeP pincer germyl metal complexes were already known before the appearance of metal-free PGeP germylenes, but the strategy used for their syntheses is not of general applicability because it involves the formation of a Ge–M bond from a Ge–C,[12,13] Ge–H,[13,14] Ge–Cl[15] or Ge–F[16] bond of a germane fragment.

The current interest in investigating TM complexes containing PGeP pincer germyl ligands is associated to the highly appreciated usefulness of pincer ligands in C–H bond activation reactions and catalysis[17,18] and to the fact that their syntheses and reactivity have so far been scarcely investigated.[2-4,8-16] In addition some PGeP pincer complexes have been satisfactorily tested as homogeneous catalyst precursors.[13,19]

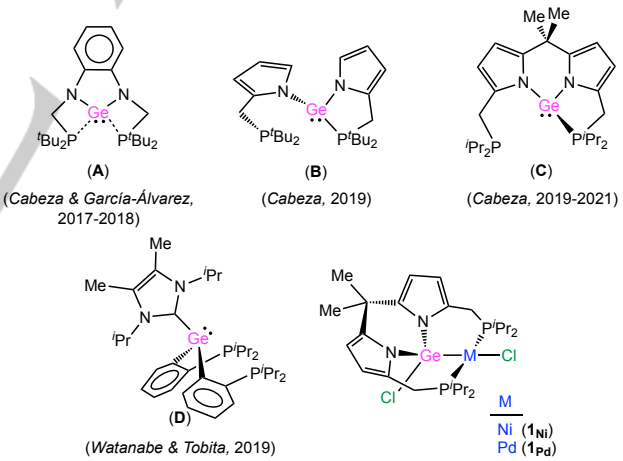

Figure 1. The currently known metal free PGeP germylenes that have led to transition metal complexes containing PGeP pincer germyl (**A**–**C**) or germylene (**C**, **D**) ligands and the PGeP pincer germyl complexes used as starting materials in this work (**1$_{Ni}$**, **1$_{Pd}$**).

In the field of PGeP pincer chemistry, we have recently shown that germylene **C** (Figure 1), which is based on the dipyrromethane scaffold,[4] is better suited than germylenes **A**[2] and **B**[3] (Figure 1) to form stable PGeP pincer chloridogermyl complexes. In fact, its nickel(II) and palladium(II) derivatives [MCl{κ^3*P*,Ge,*P*-GeCl(pyrmP^{i}Pr$_2$)$_2$CMe$_2$}], M = Ni[11] (**1$_{Ni}$**), Pd[8] (**1$_{Pd}$**); (pyrmP^{i}Pr$_2$)$_2$CMe$_2$ = 5,5'-dimethyl-2,2'-bis(di-isopropylphosphanylmethyl)dipyrromethane-1,1'-diyl; Figure 1), are undistorted square planar complexes with reasonable

thermal- and air-stability, in contrast with the related complexes derived from germylenes **A** and **B**, which present strongly distorted coordination geometries (**A** derivatives)[2,9,10] or are very air- and moisture-sensitive (**B** derivatives).[3]

We now report the first reactivity study on PGeP pincer germyl complexes derived from germylene **C**, describing the different reactivity of LiOMe and LiMe with complexes $\mathbf{1_{Ni}}$ and $\mathbf{1_{Pd}}$, which *a priori* have two chlorido ligands (in the GeCl and MCl fragments) susceptible to be substituted by other anionic nucleophiles. The regioselectivity of these reactions has been rationalized with the help of DFT calculations.

Results and Discussion

Reactivity Studies

The reactions of the PGeP pincer chloridogermyl nickel(II) and palladium(II) complexes $\mathbf{1_{Ni}}$ and $\mathbf{1_{Pd}}$ with lithium methoxide at room temperature selectively led to the methoxidogermyl derivatives [MCl{κ^3*P*,Ge,*P*-Ge(OMe)(pyrmP^{i}Pr$_2$)$_2$CMe$_2$}], M = Ni ($\mathbf{2_{Ni\text{-}OMe}}$), Pd ($\mathbf{2_{Pd\text{-}OMe}}$) (Scheme 1). Only the chloride attached to the Ge atom of $\mathbf{1_{Ni}}$ and $\mathbf{1_{Pd}}$ could be substituted, even using a three-fold excess of lithium methoxide.

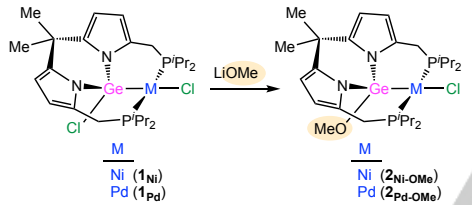

Scheme 1. Synthesis of complexes $\mathbf{2_{M\text{-}OMe}}$ (M = Ni, Pd).

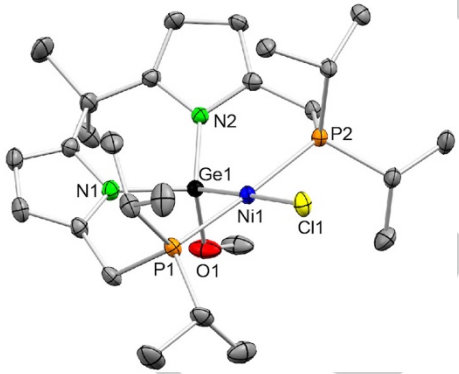

Figure 2. XRD molecular structure of complex $\mathbf{2_{Ni\text{-}OMe}}$ (30% displacement ellipsoids; H atoms have been omitted for clarity; only one of the two positions in which the OMe group is disordered is shown). Selected bond lengths (Å) and angles (°): Ni1−P1 2.208(2), Ni1−P2 2.213(2), Ni1−Cl1 2.204(2), Ni1−Ge1 2.241(2), Ge1−O1 1.82(2), Ge1−Ni1−Cl1 176.89(9), P1−Ni1−P2 176.7(1).

The C_S symmetric structure suggested by NMR (^{1}H, ^{13}C{^{1}H} and ^{31}P{^{1}H}) for complexes $\mathbf{2_{Ni\text{-}OMe}}$ and $\mathbf{2_{Pd\text{-}OMe}}$, which located the CMe$_2$ group methyls in the symmetry plane and showed diastereotopic protons for the PCH$_2$ and P^{i}Pr$_2$ groups, was confirmed by X-ray diffraction (XRD) in the case of $\mathbf{2_{Ni\text{-}OMe}}$ (Figure 2). The structure is very similar to that of its parent compound $\mathbf{1_{Ni}}$,[11] with the Ni atom in a square planar coordination and the Ge atom in a tetrahedral environment, having the Ge–Ni distance, 2.241(2) Å, slightly longer than that of $\mathbf{1_{Ni}}$, 2.2173(3) Å. Related PGeP methoxidogermyl palladium(II) and platinum(II) complexes have been previously prepared from germylene **A** (Figure 1).[9] Complex $\mathbf{2_{Ni\text{-}OMe}}$ is the first PGeP methoxidogermyl nickel(II) complex to be reported.

Both $\mathbf{1_{Ni}}$ and $\mathbf{1_{Pd}}$ reacted with methyllithium in 1:1 mol ratio to give mixtures (NMR identification) that contained some unreacted $\mathbf{1_M}$ (M = Ni, Pd) together with monomethyl [MCl{κ^3*P*,Ge,*P*-GeMe(pyrmP^{i}Pr$_2$)$_2$CMe$_2$}] ($\mathbf{2_{M\text{-}Me}}$) and dimethyl [MMe{κ^3*P*,Ge,*P*-GeMe(pyrmP^{i}Pr$_2$)$_2$CMe$_2$}] ($\mathbf{3_{M\text{-}Me}}$) reaction products (Scheme 2). The use of a 1:2 $\mathbf{1_M}$ to LiMe mole ratio allowed the complete transformation of the starting complexes $\mathbf{1_M}$ into the dimethyl derivatives $\mathbf{3_{M\text{-}Me}}$, which were isolated as pure products in high yields, proving that $\mathbf{2_{M\text{-}Me}}$ complexes are intermediates in the formation of the corresponding dimethyl products $\mathbf{3_{M\text{-}Me}}$. However, the monomethyl intermediates $\mathbf{2_{M\text{-}Me}}$ could not be satisfactorily separated from their corresponding reaction mixtures.

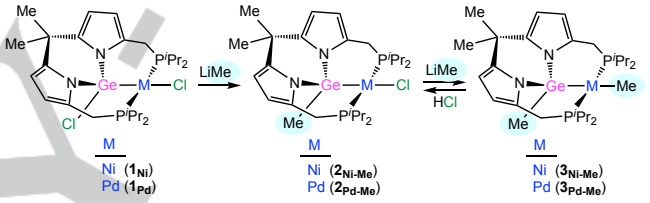

Scheme 2. Synthesis of complexes $\mathbf{2_{M\text{-}Me}}$ and $\mathbf{3_{M\text{-}Me}}$ (M = Ni, Pd).

The evasive monomethyl complexes $\mathbf{2_{M\text{-}Me}}$ (M = Ni, Pd) were satisfactorily prepared with complete selectivity by treating the dimethyl complexes $\mathbf{3_{M\text{-}Me}}$ with one equivalent of HCl (Scheme 2). No doubt, these reactions are facilitated by the very strong Lewis basicity of the PGeP pincer ligand of complexes $\mathbf{3_{M\text{-}Me}}$ (its methylgermyl and trialkylphosphane groups are very strong electron donors), which makes the corresponding M–Me fragment electron-rich enough as to be easily attacked by HCl. The loss of methane provides the corresponding monomethyl complex $\mathbf{2_{M\text{-}Me}}$.

All compounds of types $\mathbf{2_{M\text{-}Me}}$ and $\mathbf{3_{M\text{-}Me}}$ have very similar ^{1}H, ^{13}C{^{1}H} or ^{31}P{^{1}H} NMR spectra, compatible with an average C_S molecular symmetry in solution. In all cases (C_6D_6 solvent), the GeMe methyl groups are observed in the range 1.01–0.96 ppm in the ^{1}H NMR spectra and in the range 11.6–9.96 ppm in the ^{13}C{^{1}H} NMR spectra. The metal-bound methyl groups of $\mathbf{3_{M\text{-}Me}}$ appear at –0.27 (M = Ni) and 0.12 (M = Pd) ppm in the ^{1}H NMR spectra and at –11.5 (M = Ni) and –11.9 (M = Pd) ppm in the ^{13}C{^{1}H} NMR spectra. The XRD molecular structure of $\mathbf{3_{Pd\text{-}Me}}$ (Figure. 3) confirms that this complex is analogous to $\mathbf{1_{Pd}}$,[2] but now the Ge and Pd atoms are attached to methyl groups and the Ge–Pd distance, 2.3797(4) Å, is longer than that of $\mathbf{1_{Pd}}$, 2.2777(3) Å, in accordance with the stronger *trans* influence of the methyl group.

It is noteworthy that the metal coordination in $\mathbf{2_{Ni\text{-}OMe}}$, $\mathbf{3_{Pd\text{-}Me}}$ and in their precursors $\mathbf{1_{Ni}}$[9] and $\mathbf{1_{Pd}}$[2] is undistorted square planar, confirming that the formation of 6-membered MGeNC$_2$P rings in the metal complexes favors the linear coordination of the phosphane groups, which is a requirement for square planar

coordination. In contrast, related square planar complexes derived from germylene **A** display very distorted coordination geometries, with P–M–P bond angles << 180°, due to the strain imposed by their 5-membered MGeNCP metallacycle.[2,9,10]

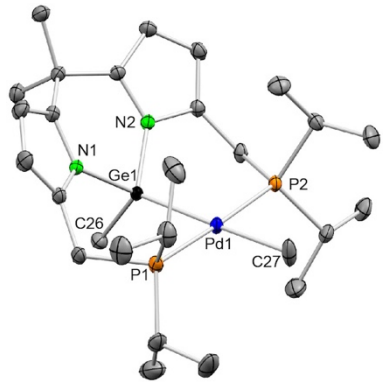

Figure 3. XRD molecular structure of complex $\mathbf{3}_{\mathbf{Pd\text{-}Me}}$ (30% displacement ellipsoids; H atoms have been omitted for clarity; only one of the two independent but analogous molecules found in the asymmetric unit is shown). Selected bond lengths (Å) and angles (°): Pd1−P1 2.2970(8), Pd1−P2 2.3001(7), Pd1−Ge1 2.3797(4), Pd1−C27 2.169(3), Ge1−C26 1.967(3), Ge1−Pd1−C27 178.4(1), P1−Pd1−P2 177.74(3).

Computational Studies

DFT calculations, at the wB97XD/SDD/cc-pVDZ level, were performed with the aim of rationalizing the experimental results.

The results described above indicate that, in the reactions of LiR (R = OMe, Me) with $\mathbf{1}_{\mathbf{M}}$ (M = Ni, Pd), the corresponding nucleophile selectively attacks the Ge atom because the reactions give the Ge-substituted products $\mathbf{2}_{\mathbf{M\text{-}R}}$. This regioselectivity can be easily explained having a look at the LUMOs of the reacting complexes (Figure 4), which contain a large contribution of the Ge atom and present an antibonding overlap between the atoms of the Ge–Cl fragment.

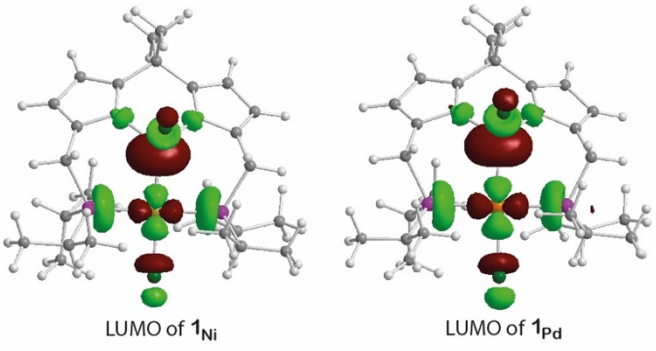

Figure 4. LUMOs of compounds $\mathbf{1}_{\mathbf{M}}$ (M = Ni, Pd; isovalue = 0.05), showing the large contribution of the Ge atom.

The contrasting reactivity presented by the monosubstituted complexes $\mathbf{2}_{\mathbf{M\text{-}OMe}}$ and $\mathbf{2}_{\mathbf{M\text{-}Me}}$ in their treatments with more LiOMe and LiMe, respectively (complexes $\mathbf{2}_{\mathbf{M\text{-}OMe}}$ remained unchanged, whereas complexes $\mathbf{2}_{\mathbf{M\text{-}Me}}$ easily ended in the dimethyl derivatives $\mathbf{3}_{\mathbf{M\text{-}Me}}$), cannot be explained by the composition of the LUMOs of $\mathbf{2}_{\mathbf{M\text{-}R}}$ (SI, Figure S21), which are very similar to those of $\mathbf{1}_{\mathbf{M}}$ (Figure 4). Therefore, other empty orbitals with energies higher than the LUMO may be involved in these reactions. It is noteworthy that the transformation of the Ge–Cl fragment of $\mathbf{2}_{\mathbf{M}}$ into the corresponding Ge–R fragment of $\mathbf{2}_{\mathbf{M\text{-}R}}$ (R = OMe, Me) is accompanied by a considerable increase of the LUMO energy and also of the nearest empty orbitals, while the energies of the corresponding HOMOs are maintained (Table 1). Interestingly, the computed energies (in the gas phase) for the HOMOs of the OMe^- and Me^- anions, –0.1837 eV and 0.9252 eV, respectively (the energies of the HOMOs of the actual nucleophiles were not computed because the actual degree of association/dissociation and solvation of LiOMe and LiMe in the reacting solutions is unknown) indicate that the mismatch between the energies of the HOMO of the nucleophile (R^-) and the LUMO of the complex increases on going from $\mathbf{1}_{\mathbf{M}}$ to $\mathbf{2}_{\mathbf{M\text{-}R}}$ for R = OMe but decreases for R = Me, confirming that, from a kinetic point of view, $\mathbf{2}_{\mathbf{M\text{-}OMe}}$ is less disposed to react with LiOMe than $\mathbf{2}_{\mathbf{M\text{-}Me}}$ with LiMe and that LiMe should react faster with $\mathbf{2}_{\mathbf{M\text{-}Me}}$ than with $\mathbf{1}_{\mathbf{M}}$. In addition, the Me^- anion is thermodynamically so reactive that it may easily substitute the M–Cl chlorido ligand, whereas the OMe^- may not.

Table 1. Energies (eV) of the frontier orbitals of complexes $\mathbf{1}_{\mathbf{M}}$ and $\mathbf{2}_{\mathbf{M\text{-}R}}$

Complex	HOMO	LUMO
$\mathbf{1}_{\mathbf{Ni}}$	–7.3438	0.3390
$\mathbf{1}_{\mathbf{Pd}}$	–7.3846	0.2199
$\mathbf{2}_{\mathbf{Ni\text{-}OMe}}$	–7.2644	0.6413
$\mathbf{2}_{\mathbf{Pd\text{-}OMe}}$	–7.3376	0.5883
$\mathbf{2}_{\mathbf{Ni\text{-}Me}}$	–7.1384	0.7741
$\mathbf{2}_{\mathbf{Pd\text{-}Me}}$	–7.2129	0.6901

Regarding the selective formation the monomethyl complexes $\mathbf{2}_{\mathbf{M\text{-}Me}}$ upon reaction of the dimethyl complexes $\mathbf{3}_{\mathbf{M\text{-}Me}}$ with HCl, we propose that these reactions should involve a protonation at either the metal (followed by reductive elimination of methane) or at the M–Me carbon atom (direct protonolysis). A concerted mechanism is less likely because it would imply the oncoming of the HCl Cl atom to the metal atom, but we know that a chloride anion is released in the reactions that lead to $\mathbf{3}_{\mathbf{M\text{-}Me}}$ from $\mathbf{2}_{\mathbf{M\text{-}Me}}$. A look at the filled molecular orbitals of complexes $\mathbf{3}_{\mathbf{M\text{-}Me}}$ (SI, Figures S22 and S23) revealed that the HOMO–3 of $\mathbf{3}_{\mathbf{Ni\text{-}Me}}$ and the HOMO–4 of $\mathbf{3}_{\mathbf{Pd\text{-}Me}}$, which are mostly constituted by the metal dz^2 orbital, are well suited to participate in a metal protonation process. Alternatively, the HOMO–2s of both $\mathbf{3}_{\mathbf{M\text{-}Me}}$ complexes might participate in C-protonation process because they have a $M–C_{Me}$ antibonding character and an appreciable contribution of the methyl C atom. Therefore, without further information, we cannot propose a reaction pathway for the hydrochlorination reactions.

Conclusions

In summary, this work describes that reactions of the dipyrromethane-based chloridogermyl PGeP pincer complexes $\mathbf{1}_{\mathbf{M}}$ (M = Ni, Pd) with LiOMe and LiMe have allowed the syntheses of new methoxidogermyl and methylgermyl PGeP pincer complexes of nickel and palladium. While LiOMe is only able to substitute the Ge-bound Cl atom of $\mathbf{1}_{\mathbf{M}}$, rendering complexes $\mathbf{2}_{\mathbf{M\text{-}OMe}}$, LiMe can also replace the two Cl atoms of $\mathbf{1}_{\mathbf{M}}$ to give the

dimethyl derivatives **3M-Me**. Although the monomethyl complexes **2M-Me** are intermediates in the syntheses of **3M-Me**, they have not been isolated from these reactions, but they have been successfully prepared by treating **3M-Me** with HCl. DFT calculations have been used to interpret the experimental results. It seems clear that the first Cl substitution on **1M** occurs on the Ge atom because the LUMOs of **1M** contain an important contribution from the Ge atom. The no reaction between **2M-OMe** and LiOMe may be explained by the fact that the LUMOs **2M-R** lie at higher energies (in the range 0.59–0.77 eV) than those of **1M** (in the range 0.22–0.34 eV) and this increases their mismatch with the energy of the HOMO of the OMe^- anion (–0.1837 eV), but not with that of the Me^- anion, which lies even higher (0.9252 eV) than those of **1M** and **2M-Me**. In addition, under a thermodynamic point of view, the Me^- anion is so reactive that it may easily substitute the M–Cl chloride anion, whereas the OMe^- may not.

Experimental Section

General Data

All reactions and product manipulations were carried out under argon in a dry box or using Schlenk-vacuum line techniques. Solvents were dried over appropriate desiccating reagents and were distilled under argon before use. Compounds **1Ni**,[11] and **1Pd**[8] were prepared following published procedures. All remaining reagents were purchased from commercial sources and were stored under argon in a dry box. All reaction products were vacuum-dried for several hours prior to being weighted and analyzed. NMR spectra were run on a Bruker NAV-400 instrument using as standards the residual protic solvent resonance for ^{1}H [δ(C_6HD_5) 7.16 ppm], the solvent resonance for ^{13}C [δ(C_6D_6) 128.10 ppm] and external 85% H_3PO_4 for ^{31}P (δ 0.00 ppm). Microanalyses were obtained with a Thermo-Finnigan FlashEA112 microanalyzer.

Synthetic Procedures and Characterization Data

[NiCl{κ^3*P*,Ge,*P*-Ge(OMe)(pyrmP^{i}Pr$_2$)$_2$CMe$_2$}] (2Ni-OMe): Solid **1Ni** (0.033 g, 0.052 mmol) was added to a methanolic solution of lithium methoxide, previously prepared from LiBu (0.094 mL, 1.6 *M* in hexanes, 0.15 mmol) and methanol (4 mL). The resulting suspension was stirred at room temperature for 12 h. Solvents were removed under vacuum and the residue was extracted into toluene (3 x 2 mL; solution decanted). The combined extracts were evaporated to dryness to give **2Ni-OMe** as a yellow solid (0.018 g, 55 %). Anal. (%): Calcd. for $C_{26}H_{45}ClGeN_2NiOP_2$ (*M* = 630.37 amu): C, 49.54; H, 7.20; N, 4.44; found**:** C, 49.68; H, 7.30; N 4.36. ^{1}H NMR (C_6D_6, 400.1 MHz, 298 K): δ 6.30 (s, 2 H, 2 C*H* of 2 pyrrole), 6.11 (s, 2 H, 2 C*H* of 2 pyrrole), 3.75 (s, 3 H, CH_3 of O*Me*), 2.82 (s, 4 H, 2 CH_2P), 2.47 (m, 2 H, 2 C*H* of 2 C*H*Me$_2$), 2.12 (m, 2 H, 2 C*H* of 2 C*H*Me$_2$), 1.87 (s, 3 H, 1 CH_3 of C*Me*$_2$), 1.81 (s, 3 H, 1 CH_3 of C*Me*$_2$), 1.47 (m, 6 H, 2 CH_3 of 2 CH*Me*$_2$), 1.13 (m, 6 H, 2 CH_3 of 2 CH*Me*$_2$), 0.94 (m, 6 H, 2 CH_3 of 2 CH*Me*$_2$), 0.82 (m, 6 H, 2 CH_3 of 2 CH*Me*$_2$) ppm. ^{13}C{^{1}H} NMR (C_6D_6, 100.6 MHz, 298 K): δ 145.7 (s, 2 *C* of 2 pyrrole), 108.8 (s, 2 *C*H of 2 pyrrole), 104.8 (s, 2 *C*H of 2 pyrrole), 52.9 (s, *C*H$_3$ of O*Me*), 39.4 (s, 1 *C*H$_3$ of C*Me*$_2$), 37.0 (s, *C*Me$_2$), 27.6 (s, 1 *C*H$_3$ of C*Me*$_2$), 27.0 (vt, $J_{C\text{-}P}$ = 10.8 Hz, 2 *C*H of 2 *C*HMe$_2$), 24.9 (vt, $J_{C\text{-}P}$ = 10.8 Hz, 2 *C*H of 2 *C*HMe$_2$), 20.2 (vt, $J_{C\text{-}P}$ = 12.1 Hz, 2 *C*H$_2$P), 19.9 (s, 2 *C*H$_3$ of 2 CH*Me*$_2$), 19.9 (s, 2 *C*H$_3$ of 2 CH*Me*$_2$), 18.1 (s, 2 *C*H$_3$ of 2 CH*Me*$_2$), 17.8 (s, 2 *C*H$_3$ of 2 CH*Me*$_2$) ppm. ^{31}P{^{1}H} NMR (C_6D_6, 162.1 MHz, 298 K): δ 35.7 (s) ppm.

[PdCl{κ^3*P*,Ge,*P*-Ge(OMe)(pyrmP^{i}Pr$_2$)$_2$CMe$_2$}] (2Pd-OMe): Solid **1Pd** (0.10 g, 0.15 mmol) was added to a methanolic solution of lithium methoxide, previously prepared from LiBu (0.21 mL, 1.6 *M* in hexanes, 0.33 mmol) and methanol (6 mL). The resulting suspension was stirred at room temperature for 12 h. Solvents were removed under vacuum and the residue was extracted into toluene (4 x 3 mL; solution decanted). The combined extracts were evaporated to dryness to give **2Pd-OMe** as a yellow solid (0.69 g, 68 %). Anal. (%): Calcd. for $C_{26}H_{45}ClGeN_2OP_2Pd$ (*M* = 678.09 amu): C, 46.05; H, 6.69; N, 4.13; found**:** C, 46.11; H, 6.77; N 4.09. ^{1}H NMR (C_6D_6, 400.1 MHz, 298 K): δ 6.28 (s, 2 H, 2 C*H* of 2 pyrrole), 6.10 (s, 2 H, 2 C*H* of 2 pyrrole), 3.75 (s, 3 H, CH_3 of O*Me*), 2.95 (d, 2 H, $J_{H\text{-}H}$ = 14.5 Hz, 2 C*H* of 2 CH_2P), 2.87 (d, 2 H, $J_{H\text{-}H}$ = 14.5 Hz, 2 C*H* of 2 CH_2P), 2.54 (m, 2 H, 2 C*H* of 2 C*H*Me$_2$), 2.17 (m, 2 H, 2 C*H* of 2 C*H*Me$_2$), 1.84 (s, 6 H, 2 CH_3 of C*Me*$_2$), 1.35 (m, 6 H, 2 CH_3 of 2 CH*Me*$_2$), 1.09 (m, 6 H, 2 CH_3 of CH*Me*$_2$), 0.89 (m, 6 H, 2 CH_3 of 2 CH*Me*$_2$), 0.72 (m, 6 H, 2 CH_3 of CH*Me*$_2$) ppm. ^{13}C{^{1}H} NMR (C_6D_6, 100.6 MHz, 298 K): δ 146.0 (s, 2 *C* of 2 pyrrole), 109.5 (s, 2 *C*H of 2 pyrrole), 104.6 (s, 2 *C*H of 2 pyrrole), 53.1 (s, *C*H$_3$ of O*Me*), 39.3 (s, 1 *C*H$_3$ of C*Me*$_2$), 37.0 (s, *C*Me$_2$), 27.4 (vt, $J_{C\text{-}P}$ = 10.8 Hz, 2 *C*H of 2 *C*HMe$_2$), 26.4 (s, 1 *C*H$_3$ of C*Me*$_2$), 24.8 (vt, $J_{C\text{-}P}$ = 11.5 Hz, 2 *C*H of 2 *C*HMe$_2$), 20.6 (vt, $J_{C\text{-}P}$ = 11.5 Hz, 2 *C*H$_2$P), 19.9 (s, 2 *C*H$_3$ of 2 CH*Me*$_2$), 19.6 (s, 2 *C*H$_3$ of 2 CH*Me*$_2$), 18.3 (s, 2 *C*H$_3$ of 2 CH*Me*$_2$), 17.8 (s, 2 *C*H$_3$ of 2 CH*Me*$_2$) ppm. ^{31}P{^{1}H} NMR (C_6D_6, 162.1 MHz, 298 K): δ 39.4 (s) ppm.

1:1 reaction of 1Ni with LiMe: LiMe (50 µL, 1.6 M in diethyl ether, 0.080 mmol) was added to a suspension of **1Ni** (0.051 g, 0.080 mmol) in toluene. The resulting orange suspension was stirred for 2 h. Solvents were removed under vacuum and the residue was extracted into toluene (3 x 3 mL; solution decanted). The combined extracts were evaporated to dryness to give a solid containing a 5:1:2 mixture of **1Ni**, **2Ni-Me** and **3Ni-Me** (^{31}P{^{1}H} NMR analysis, C_6D_6) that could not be separated.

1:1 reaction of 1Pd with LiMe: MeLi (50 µL, 1.6 M in diethyl ether, 0.080 mmol) was added to a suspension of **1Pd** (0.055 g, 0.080 mmol) in toluene. The resulting orange suspension was stirred for 2 h. The solvents were removed under vacuum and the residue was extracted into toluene (3 x 3 mL; solution decanted). The combined extracts were evaporated to dryness to give a solid containing a 4:1:3 mixture of **1Pd**, **2Pd-Me** and **3Pd-Me** (^{31}P{^{1}H} NMR analysis, C_6D_6) that could not be separated.

[NiMe{κ^3*P*,Ge,*P*-GeMe(pyrmP^{i}Pr$_2$)$_2$CMe$_2$}] (3Ni-Me): LiMe (0.14 mL, 1.6 *M* in diethyl ether, 0.22 mmol) was added to a solution of **1Ni** (0.060 g, 0.10 mmol) in toluene (6 mL). The resulting orange suspension was stirred at room temperature for 4 h. Solvents were removed under vacuum and the residue was extracted into toluene (3 x 5 mL; solution decanted). The combined extracts were evaporated to dryness to give **3Ni-Me** as a dark orange solid (0.047 g, 82 %). Anal. (%): Calcd. for $C_{27}H_{48}GeN_2NiP_2$ (*M* = 593.95 amu): C, 54.60; H, 8.15; N, 4.72; found: C, 54.71; H, 8.23; N 4.63. ^{1}H NMR (C_6D_6, 400.1 MHz, 298 K): δ 6.44 (d, $J_{H\text{-}H}$ = 4.0 Hz, 2 H, 2 C*H* of 2 pyrrole), 6.24 (s, br, 2 H, 2 C*H* of 2 pyrrole), 3.04 (m, 2 H, 2 C*H* of 2 CH_2P), 2.56 (d, $J_{H\text{-}H}$ = 16.0 Hz, 2 H, 2 C*H* of 2 CH_2P), 2.05 (m, 2 H, 2 C*H* of 2 C*H*Me$_2$), 1.99 (s, 3 H, 1 CH_3 of C*Me*$_2$), 1.91 (m, 2 H, 2 C*H* of 2 C*H*Me$_2$), 1.83 (s, 3 H, 1 CH_3 of C*Me*$_2$), 1.12 (dd, $J_{H\text{-}P}$= 16.0 Hz, $J_{H\text{-}H}$ = 8.0 Hz, 6 H, 2 CH_3 of 2 CH*Me*$_2$), 0.96 (s, 3 H, CH_3 of Ge*Me*), 0.92–0.80 (m, 18 H, 6 CH_3 of 6 CH*Me*$_2$), –0.28 (t, $J_{H\text{-}H}$ = 7.8 Hz, 3 H, CH_3 of Ni*Me*) ppm.^{13}C{^{1}H} NMR (C_6D_6, 100.6 MHz, 298 K): δ 145.1 (s, 2 *C* of 2 pyrrole), 107.5 (s, 2 *C*H of 2 pyrrole), 103.5 (s, 2 *C*H of 2 pyrrole), 39.5 (s, 1 *C*H$_3$ of C*Me*$_2$), 37.0 (s, *C*Me$_2$), 26.9 (vt, $J_{C\text{-}P}$ = 9.9 Hz, 2 *C*H of 2 *C*HMe$_2$), 26.2 (s, 1 *C*H$_3$ of C*Me*$_2$), 24.7 (vt, $J_{C\text{-}P}$ = 9.9 Hz, 2 *C*H of 2 *C*HMe$_2$), 21.5 (vt, $J_{C\text{-}P}$ = 11.3 Hz, 2 *C*H$_2$P), 20.2 (s, 2 *C*H$_3$ of 2 CH*Me*$_2$), 20.1 (s, 2 *C*H$_3$ of 2 CH*Me*$_2$), 18.2 (s, 2 *C*H$_3$ of 2 CH*Me*$_2$), 18.0 (s, 2 *C*H$_3$ of 2 CH*Me*$_2$), 10.6 (s, *C*H$_3$ of Ge*Me*), –11.5 (t, $J_{C\text{-}P}$ = 20.6 Hz, *C*H$_3$ of Ni*Me*) ppm. ^{31}P{^{1}H} NMR (C_6D_6, 162.1 MHz, 298 K): δ 43.2 (s) ppm.

[PdMe{κ^3*P*,Ge,*P*-GeMe(pyrmP^{i}Pr$_2$)$_2$CMe$_2$}] (3Pd-Me): LiMe (0.19 mL, 1.6 *M* in diethyl ether, 0.30 mmol) was added to a solution of **1Pd** (0.090 g, 0.14 mmol) in toluene (6 mL). The resulting orange suspension was stirred at room temperature for 4 h. Solvents were removed under vacuum and the residue was extracted into toluene (3 x 5 mL; solution decanted). The combined extracts were evaporated to dryness to give **3Pd-Me** as a dark orange solid (0.077 g, 86 %). Anal. (%): Calcd. for $C_{27}H_{48}GeN_2P_2Pd$ (*M* = 641.67 amu): C, 50.54; H, 7.54; N, 4.37; found**:** C, 50.61; H, 7.64; N 4.29. ^{1}H NMR (C_6D_6, 400.1 MHz, 298 K): δ 6.42 (s, 2 H, 2 C*H* of 2 pyrrole), 6.24 (s, 2 H, 2 C*H* of 2 pyrrole), 3.20 (d, $J_{H\text{-}H}$ = 14.5 Hz, 2 H, 2 C*H* of 2 CH_2P), 2.64 (d, $J_{H\text{-}H}$ = 14.5 Hz, 2 H, 2 C*H* of 2 CH_2P), 2.01–1.94 (m, 7 H, 1 CH_3 of

1 C*Me*$_2$ + 4 C*H* of 4 C*H*Me$_2$), 1.85 (s, 3 H, 1 C*H*$_3$ of C*Me*$_2$) 1.06 (dd, 6 H, J_{H-H}= 6.0 Hz, J_{H-P}= 14.0 Hz, 2 C*H*$_3$ of 2 CH*Me*$_2$), 1.01 (s, 3 H, C*H*$_3$ of Ge*Me*), 0.92–0.74 (m, 18 H, 6 C*H*$_3$ of 6 CH*Me*$_2$), 0.12 (t, J_{H-P} = 5.3 Hz, 3 H, C*H*$_3$ of Pd*Me*) ppm. ^{13}C{^{1}H} NMR (C_6D_6, 100.6 MHz, 298 K): δ 145.3 (s, 2 *C* of 2 pyrrole), 108.2 (s, 2 *C*H of 2 pyrrole), 103.4 (s, 2 *C*H of 2 pyrrole), 39.0 (s, 1 CH$_3$ of C*Me*$_2$), 37.0 (s, C*Me*$_2$), 26.4 (vt, J_{C-P} = 10.7 Hz, 2 *C*H of 2 *C*HMe$_2$),26.2 (s, 1 CH$_3$ of C*Me*$_2$),25.0 (vt, J_{C-P} = 10.7 Hz, 2 *C*H of 2 *C*HMe$_2$), 22.5 (vt, J_{C-P} = 11.6 Hz, 2 *C*H$_2$P), 19.7 (s, 2 CH$_3$ of 2 CH*Me*$_2$), 19.6 (s, 2 *C*H$_3$ of 2 CH*Me*$_2$), 18.2 (s, 2 *C*H$_3$ of 2 CH*Me*$_2$), 17.9 (s, 2 *C*H$_3$ of 2 CH*Me*$_2$), 11.6 (s, *C*H$_3$ of Ge*Me*), –11.9 (t, J_{C-P} = 8.4 Hz, *C*H$_3$ of Pd*Me*) ppm. ^{31}P{^{1}H} NMR (C_6D_6, 162.1 MHz, 298 K): δ 42.7 (s) ppm.

[NiCl{κ^3*P*,Ge,*P*-GeMe(pyrmP^{i}Pr$_2$)$_2$CMe$_2$}] (2$_{Ni-Me}$): HCl (61 µL, 1.0 *M* in diethyl ether, 0.061 mmol) was added to a solution of **3$_{Ni-Me}$** (0.030 g, 0.051 mmol) in toluene (5 mL). The resulting orange solution was stirred at room temperature for 2 h and was evaporated to dryness to give **2$_{Ni-Me}$** as an orange solid (0.020 g, 64 %). Anal. (%): Calcd. for $C_{26}H_{45}ClGeN_2NiP_2$ (*M* = 614.37 amu): C, 50.83; H, 7.38; N, 4.56; found**:** C, 50.91; H, 7.44; N 4.52. ^{1}H NMR (C_6D_6, 400.1 MHz, 298 K): δ 6.37 (s, 2 H, 2 C*H* of 2 pyrrole), 6.15 (s, 2 H, 2 C*H* of 2 pyrrole), 2.81 (d, J_{H-H} = 13.8 Hz, 2 H, 2 C*H* of 2 C*H*$_2$P), 2.55 (m, 2 H, 2 C*H* of 2 C*H*Me$_2$), 2.44 (d, J_{H-H} = 13.8 Hz, 2H, 2 C*H* of 2 C*H*$_2$P), 2.16 (m, 2 H, 2 C*H* of 2 C*H*Me$_2$), 1.92 (s, 3 H, 1 C*H*$_3$ of C*Me*$_2$), 1.67 (s, 3 H, 1 C*H*$_3$ of C*Me*$_2$), 1.39 (m, 2 C*H*$_3$ of 2 CH*Me*$_2$), 1.16 (m, 2 C*H*$_3$ of 2 CH*Me*$_2$), 0.97 (s, 3 H, C*H*$_3$ of Ge*Me*), 0.87 (m, 12 H, 4 C*H*$_3$ of 4 CH*Me*$_2$) ppm. ^{13}C{^{1}H} NMR (C_6D_6, 100.6 MHz, 298 K): δ 144.7 (s, 2 *C* of 2 pyrrole), 108.3 (s, 2 *C*H of 2 pyrrole), 104.3 (s, 2 *C*H of 2 pyrrole), 39.9 (s, 1 *C*H$_3$ of C*Me*$_2$), 36.9 (s, *C*Me$_2$), 27.3 (vt, J_{C-P} = 11.0 Hz, 2 *C*H of 2 *C*HMe$_2$), 26.2 (s, 1 *C*H$_3$ of C*Me*$_2$), 24.7 (vt, J_{C-P} = 11.0 Hz, 2 *C*H of 2 *C*HMe$_2$), 20.1 (s, 2 *C*H$_3$ of 2 CH*Me*$_2$), 20.0 (s, 2 *C*H$_3$ of 2 CH*Me*$_2$), 19.7 (vt, J_{C-P} = 11.2 Hz, 2 *C*H$_2$P), 18.3 (s, 2 *C*H$_3$ of 2 CH*Me*$_2$), 17.7 (s, 2 *C*H$_3$ of 2 CH*Me*$_2$), 9.9 (t, J_{C-P} = 5.0 Hz, *C*H$_3$ of Ge*Me*) ppm. ^{31}P{^{1}H} NMR (C_6D_6, 162.1 MHz, 298 K): δ 37.8 (s) ppm.

[PdCl{κ^3*P*,Ge,*P*-GeMe(pyrmP^{i}Pr$_2$)$_2$CMe$_2$}] (2$_{Pd-Me}$): HCl (61 µL, 1.0 *M* in diethyl ether, 0.061 mmol) was added to a solution of **3$_{Pd-Me}$** (0.030 g, 0.047 mmol) in toluene (5 mL). The resulting orange solution was stirred at room temperature for 2 h and was evaporated to dryness to give **2$_{Pd-Me}$** as dark yellow solid (0.021 g, 66%). Anal.(%): Calcd. for $C_{26}H_{45}ClGeN_2P_2Pd$ (*M* = 662.09 amu): C, 47.17; H, 6.85; N, 4.23; found**:** C, 47.21; H, 6.93; N 4.17. ^{1}H NMR (C_6D_6, 400.1 MHz, 298 K): δ 6.33 (s, 2 H, 2 C*H* of 2 pyrrole), 6.15 (s, 2 H, 2 C*H* of 2 pyrrole), 2.95 (d, J_{H-H} = 14.6 Hz, 2 H, 2 C*H* of 2 C*H*$_2$P), 2.59 (m, 2 H, 2 C*H* of 2 C*H*Me$_2$), 2.53 (d, J_{H-H} = 14.6 Hz, 2 H, 2 C*H* of 2 C*H*$_2$P), 2.21 (m, 2 H, 2 C*H* of 2 C*H*Me$_2$), 1.89 (s, 3 H, 1 C*H*$_3$ of C*Me*$_2$), 1.66 (s, 3 H, 1 C*H*$_3$ of C*Me*$_2$), 1.32 (dd, J_{H-P} = 14.0 Hz, J_{H-H} = 6.0 Hz, 6 H, 2 C*H*$_3$ of 2 CH*Me*$_2$), 1.13 (dd, J_{H-P} = 14.0 Hz, J_{H-H} = 6.0 Hz, 6 H, 2 C*H*$_3$ of CH*Me*$_2$), 0.98 (s, 3 H, C*H*$_3$ of Ge*Me*), 0.88 (dd, J_{H-P} = 14.0 Hz, J_{H-H} = 6.0 Hz, 6 H, 2 C*H*$_3$ of 2 CH*Me*$_2$), 0.77 (dd, J_{H-P} = 14.0 Hz, J_{H-H} = 6.0 Hz, 6 H, 2 C*H*$_3$ of 2 CH*Me*$_2$) ppm. ^{13}C{^{1}H} NMR (C_6D_6, 100.6 MHz, 298 K): δ 144.8 (s, 2 *C* of 2 pyrrole), 109.0 (s, 2 *C*H of 2 pyrrole), 104.3 (s, 2 *C*H of 2 pyrrole), 39.6 (s, 1 *C*H$_3$ of C*Me*$_2$), 36.9 (s, *C*Me$_2$), 27.3 (vt, J_{C-P} = 11.6 Hz, 2 *C*H of 2 *C*HMe$_2$), 26.0 (s, 1 *C*H$_3$ of C*Me*$_2$), 24.8 (vt, J_{C-P} = 11.6 Hz, 2 *C*H of 2 *C*HMe$_2$), 20.1–19.8 (m, 2 *C*H$_2$P + 4 *C*H$_3$ of 4 CH*Me*$_2$), 18.3 (s, 2 *C*H$_3$ of 2 CH*Me*$_2$), 17.8 (s, 2 *C*H$_3$ of 2 CH*Me*$_2$), 11.3 (t, J_{C-P} = 4.4 Hz, *C*H$_3$ of Ge*Me*) ppm. ^{31}P{^{1}H} NMR (C_6D_6, 162.1 MHz, 298 K): δ 42.8 (s) ppm.

X-ray Diffraction Analyses

Crystals of **2$_{Ni-OMe}$** and **3$_{Pd-Me}$** were analyzed by X-ray diffraction. A selection of crystal, measurement and refinement data is given in Table S1. Diffraction data were collected on an Oxford Diffraction Xcalibur Onyx Nova single crystal diffractometer with CuKα radiation. Empirical absorption corrections were applied using the SCALE3 ABSPACK algorithm as implemented in CrysAlisPro RED.[20] The structures were solved using SIR-97.[21] Isotropic and full matrix anisotropic least square refinements were carried out using SHELXL.[22] The atoms of the OMe group of **2$_{Ni-OMe}$** were found disordered into two position with a 50% occupancy and were refined isotropically. Two independent molecules were found in the asymmetric unit of **3$_{Pd-Me}$**. Unless otherwise stated the non-H atoms were refined anisotropically. H atoms were set in calculated positions and were refined riding on their parent atoms. The WINGX program system[23] was used throughout the structure determinations. The molecular plots were made with MERCURY.[24] CCDC deposition numbers: 2057748 (**2$_{Ni-OMe}$**), 2057749 (**3$_{Pd-Me}$**).

Computational Details

Structure optimizations were performed with the Gaussian09[25] suite of programs, using the wB97XD6[26] functional, which includes the second generation of Grimme's dispersion interaction correction.[27] The Stuttgart–Dresden relativistic effective core potential and the associated basis sets (SDD) were used for the Ni[28] and Pd[29] atoms. The cc-pVDZ basis set[30] was used for the remaining atoms. Frequency calculations confirmed the optimized structures as energy minima (zero imaginary eigenvalues).

Acknowledgements

This work has been supported by Ministerio de Economía y Competitividad (CTQ2016-75218-P and RED2018-102387-T) and Agencia Estatal de Investigación (PID2019-104652GB-100) research grants. The authors also acknowledge the technical support provided by *Servicios Científico-Técnicos de la Universidad de Oviedo*.

Keywords: PGeP pincers • germylenes • germyl ligands • nickel • palladium

[1] For a review, see: J. A. Cabeza, P. García-Álvarez, C. J. Laglera-Gándara, *Eur. J. Inorg. Chem*. **2020**, 784–795.
[2] L. Álvarez-Rodríguez, J. Brugos, J. A. Cabeza, P. García-Álvarez, E. Pérez-Carreño, D. Polo, *Chem. Commun*. **2017**, *53*, 893–896.
[3] J. A. Cabeza, I. Fernández, J. M. Fernández-Colinas, P. García-Álvarez, C. J. Laglera-Gándara, *Chem. Eur. J.* **2019**, *25*, 12423–12430.
[4] J. A. Cabeza, I. Fernández, P. García-Álvarez, C. J. Laglera-Gándara, *Dalton Trans.* **2019**, *48*, 13273–13280.
[5] S. Bestgen, N. H. Rees, J. M. Goicoechea, *Organometallics* **2018**, *37*, 4147–4155.
[6] S. Bestgen, M. Metha, T. C. Johnstone, P. W. Roesky, J. M. Goicoechea, *Chem. Eur. J*. **2020**, *26*, 9024–9034.
[7] T. Watanabe, Y. Kasai, H. Tobita, *Chem. Eur. J*. **2019**, *25*, 13491–13495.
[8] J. A. Cabeza, P. García-Álvarez, C. J. Laglera-Gándara, E. Pérez-Carreño, *Chem. Commun.* **2020**, *56*, 14095–14097.
[9] L. Álvarez-Rodríguez, J. Brugos, J. A. Cabeza, P. García-Álvarez, E. Pérez-Carreño, *Chem. Eur. J.* **2017**, *23*, 15107–15115.
[10] J. Brugos, J. A. Cabeza, P. García-Álvarez, E. Pérez-Carreño, D. Polo, *Organometallics* **2018**, *37*, 1507–1514.
[11] A. Azauzo, J. A. Cabeza, I. Fernández, P. García-Álvarez, I. García-Rubio, C. J. Laglera-Gándara, *Chem. Eur. J.* **2021**, *27*, 4985–4992.
[12] H. Kameo, S. Ishi, H. Nakazawa, *Dalton Trans.* **2012**, *41*, 11386–11392.
[13] J. Takaya, S. Nakamura, N. Iwasawa, *Chem. Lett.* **2012**, *41*, 967–969.
[14] J. Takaya, N. Iwasawa, *Eur. J. Inorg. Chem*. **2018**, 5012–5018.
[15] H. Kameo, K. Ikeda, S. Sakaki, S. Takemoto, H. Nakazawa, H. Matsuzaka, *Dalton Trans.* **2016**, *45*, 7570–7580.
[16] H. Kameo, K. Ikeda, D. Bourissou, S. Sakaki, S. Takemoto, H. Nakazawa, H. Matsuzaka, *Organometallics* **2016**, *35*, 713–719.
[17] For selected recent reviews on pincer complexes and their applications, see: a) E. Peris, R. H. Crabtree, *Chem. Soc. Rev*. **2018**, *47*, 1959–1968; b) *The Privileged Pincer–Metal Platform: Coordination Chemistry & Applications*, (Eds. G. van Koten, R. A. Gossage), Springer, Cham, **2016**; c) M. Asay, D. Morales-Morales, *Dalton Trans*. **2015**, *44*, 17432–17477; d) C. Gunanathan, D. Milstein,

Chem. Rev. **2014**, *114*, 12024–12087; e) *Organometallic Pincer Chemistry*, (Eds. G. van Koten, D. Milstein), Springer, Heidelberg, **2013**; f) S. Schneider, J. Meiners, B. Askevold, *Eur. J. Inorg. Chem*. **2012**, 412-429.

[18] For selected reviews on pincer complexes in homogeneous catalysis, see: a) G. Bauer, X. Hu, *Inorg. Chem. Front*. **2016**, **3**, 741–765; b) H. A. Yonus, W. Su, N. Ahmad, S. Chen, F. Verpoort, *Adv. Synth. Catal*. **2015**, *357*, 283–330; c) *Pincer and Pincer-Type Complexes: Applications in Organic Synthesis and Catalysis*, (Eds. K. J. Szabó, O. F. Wendt), Wiley-VCH, Weinheim, **2014**; d) Q.-H. Dend, R. L. Melen, L. H. Gade, *Acc. Chem. Res*. **2014**, *47*, 3162–3173.

[19] C. Zhu, J. Takaya, N. Iwasawa, *Org. Lett.* **2015**, *17*, 1814–1817.

[20] *CrysAlisPro RED*, version 1.171.38.43, Rigaku Oxford Diffraction Ltd., Oxford, UK, **2015**.

[21] A. Altomare, M. C. Burla, M. Camalli, G. Cascarano, C. Giacovazzo, A. Guagliardi, A. G. C. Moliterni, G. Polidori, R. Spagna, *J. Appl. Cryst.* **1999**, *32*, 115–119.

[22] *SHELXL-2014*: G. M. Sheldrick, *Acta Cryst.* **2008**, *A64*, 112–122.

[23] *WINGX*, version 2013.3: L. J. Farrugia, *J. Appl. Cryst.* **2012**, *45*, 849–854.

[24] *MERCURY,* version 2020.3.0, Cambridge Crystallographic Data Centre, Cambridge, UK, **2020**.

[25] M. J. Frisch, G. W. Trucks, H. B. Schlegel, G. E. Scuseria, M. A. Robb, J. R. Cheeseman, G. Scalmani, V. Barone, B. Mennucci, G. A. Petersson, H. Nakatsuji, M. Caricato, X. Li, H. P. Hratchian, A. F. Izmaylov, J. Bloino, G. Zheng, J. L. Sonnenberg, M. Hada, M. Ehara, K. Toyota, R. Fukuda, J. Hasegawa, M. Ishida, T. Nakajima, Y. Honda, O. Kitao, H. Nakai, T. Vreven, J. A. Montgomery Jr., J. E. Peralta, F. Ogliaro, M. Bearpark, J. J. Heyd, E. Brothers, K. N. Kudin, V. N. Staroverov, R. Kobayashi, J. Normand, K. Raghavachari, A. Rendell, J. C. Burant, S. S. Iyengar, J. Tomasi, M. Cossi, N. Rega, N. J. Millam, M. Klene, J. E. Knox, J. B. Cross, V. Bakken, C. Adamo, J. Jaramillo, R. Gomperts, R. E. Stratmann, O. Yazyev, A. J. Austin, R. Cammi, C. Pomelli, J. W. Ochterski, R. L. Martin, K. Morokuma, V. G. Zakrzewski, G. A. Voth, P. Salvador, J. J. Dannenberg, S. Dapprich, A. D. Daniels, Ö. Farkas, J. B. Foresman, J. V. Ortiz, J. Cioslowski, D. J. Fox, *Gaussian 09*, Revision A.01, Gaussian, Inc., Wallingford, CT, **2009**.

[26] J.-D. Chai, M. Head-Gordon, *Phys. Chem. Chem. Phys*. **2008**, *10*, 6615–6620.

[27] a) S. Ehrlich, J. Moellmann, S. Grimme, *Acc. Chem. Res*. **2013**, *46*, 916–926; b) S. Grimme, *Comput. Mol. Sci.*, **2011**, *1*, 211–228; c) T. Schwabe, S. Grimme, *Acc. Chem. Res*. **2008**, *41*, 569–579.

[28] a) M. Dolg, U. Wedig, H. Stoll, H. Preuss, *J. Chem. Phys.***1987**, *86*, 866–878; b) J. M. L. Martin, A. Sundermann, *J. Chem. Phys.* **2001**, *114*, 3408–3420.

[29] K. A. Peterson, D. Figgen, M. Dolg, H. Stoll, *J. Chem. Phys.* **2007**, *126*, 124101-1–124101-12.

[30] T. H. Dunning, *J. Chem. Phys.* **1989**, *90*, 1007–1023.

Entry for the Table of Contents

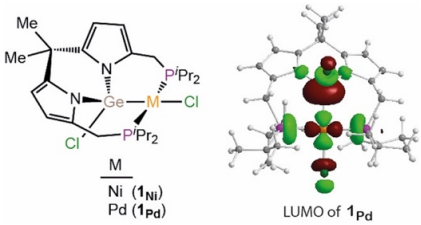

While LiOMe is only able to substitute the Ge–Cl chlorido ligand of the PGeP pincer germyl complexes **1**$_{Ni}$ and **1**$_{Pd}$, LiMe is able to sequentially substitute first the Ge–Cl and then the M–Cl chlorido ligands. The regioselectivity of these reactions is orbital-controlled because the LUMO of the dichlorido complexes contains an important contribution of the Ge atom.

Institute and/or researcher Twitter usernames: @uniovi_info @ja_cabeza

ORCID Identifiers

Javier A. Cabeza http://orcid.org/0000-0001-8563-9193

Pablo García-Álvarez http://orcid.org/0000-0002-5024-3874

Carlos J. Laglera-Gándara http://orcid.org/0000-0002-4480-1315

Enrique Pérez-Carreño http://orcid.org/0000-0001-8042-0678